Small-scale testing of laterally loaded monopiles in sand

K. Thomassen, H.R. Roesen, L.B. Ibsen & S.P.H. Sørensen
Department of Civil Engineering – Aalborg University, Aalborg, Denmark

2011 Pan-Am CGS Geotechnical Conference

ABSTRACT
In current designs of offshore wind turbines, monopiles are often used as foundation. The behaviour of the monopiles when subjected to lateral loading has not been fully investigated. In this paper, the behaviour of two non-slender piles in sand subjected to lateral loading are analysed by means of small-scale laboratory tests. Six quasi-static tests are conducted on piles with diameters of 40mm and 100mm and a slenderness ratio, L/D, of 5. To minimise scale effects, the tests are carried out in a pressure tank at various stress levels. From the obtained load-deflection relationships it is revealed that the uncertainties of the results for the pile with a diameter of 40mm are large. The load-deflection relationships normalised as $H/(L^2D\gamma')$ and y/D indicate that the lateral load, H, is proportional to L^2D. Comparison of the normalised load-deflection relationships for different stress levels shows that small-scale tests applied with overburden pressure are preferable.

PRESENTACIONES TÉCNICAS
En el diseño actual de turbinas eólicas marinas, mono-pilas son normalmente usadas como cimentación. El comportamiento de las mono-pilas cuando están sometidas a cargas laterales no ha sido completamente investigado a fecha de hoy. En este artículo, el comportamiento de dos mono-pilas no esbeltas instaladas en arena sometidas a cargas laterales es analizado mediante tests de laboratorio a escala reducida. Seis tests cuasi-estáticos son realizados sobre mono-pilas con diámetros de 40mm y 100 mm y relación de esbeltez de 5. Para minimizar los efectos de escala, los tests son llevados a cabo en un tanque de presión a diferentes niveles de presión. De la relación fuerza-desplazamiento obtenida, se puede concluir que las incertidumbres de los resultados de la mono-pila con diámetro de 40 mm son mayores. Las relaciones fuerza-desplazamiento normalizadas como $H/(L^2D\gamma')$ y *y/D indican que la carga lateral H es proporcional a L^2D*. Una comparación de las relaciones fuerza-desplazamiento normalizadas para diferentes niveles de presión muestra que los tests a pequeña escala con presión extra aplicada son preferibles.

1 INTRODUCTION

In the design of laterally loaded monopiles, the *p–y* curve method given in the design regulations API (1993) and DNV (1992) is often used. For piles in sand, the recommended *p–y* curves are based on results from two slender, flexible piles with a slenderness ratio $L/D = 34.4$ where L is the embedded length and D is the diameter. Contrary to the assumption of flexible piles for these curves, the monopile foundations installed today have a slenderness ratio $L/D < 10$, and behave almost as rigid objects. The recommended curves do not take the effect of the slenderness ratio into account. Furthermore, the initial stiffness is considered independent of the pile properties such as the pile diameter. The research within the field of diameter effects gives contradictory conclusions. Different studies have shown the initial stiffness to be either independent, linearly dependent, or non-linear dependent on the pile diameter, cf. Brødbæk et al. (2009).

This paper evaluates the effects of the pile diameter on the soil resistance through six small-scale tests.

2 TEST PROGRAMME

Scale effects occur when conducting small-scale tests in sand at 1 g. At low stress levels, the soil parameters, in particular the internal angle of friction, will vary strongly with the effective stresses. Therefore, it is an advantage to increase the effective stresses to a level where the internal angle of friction is independent of the stress variations. This increase in stresses will minimize the fluctuations of the measurements as well. In order to make the increase in stress level possible, the tests are conducted in a pressure tank.

The tests are carried out at stress levels of 0 kPa, 50 kPa, and 100 kPa, respectively, and the results are presented in this paper. The tests are quasi-static tests on two closed ended aluminium pipe piles with outer diameters of 40 mm and 100 mm and a slenderness ratio of 5, corresponding to embedded lengths of 200 mm and 500 mm, respectively. The wall thickness of the piles is 5 mm.

The test programme, cf. Table 1, is designed to investigate the soil resistance dependency of the pile diameter at different stress levels. The pile diameters in the test programme are chosen to supplement the tests described in Sørensen et al. (2009) where piles with diameters of 60 mm and 80 mm were tested. To some extent, the results from these tests are included in this paper.

Table 1. The test programme.

	Diameter *D* [mm]	Slenderness ratio *L/D* [-]	Overburden pressure P_0 [kPa]
Test 1	100	5	0
Test 2	100	5	50
Test 3	100	5	100
Test 4	40	5	0
Test 5	40	5	50
Test 6	40	5	100

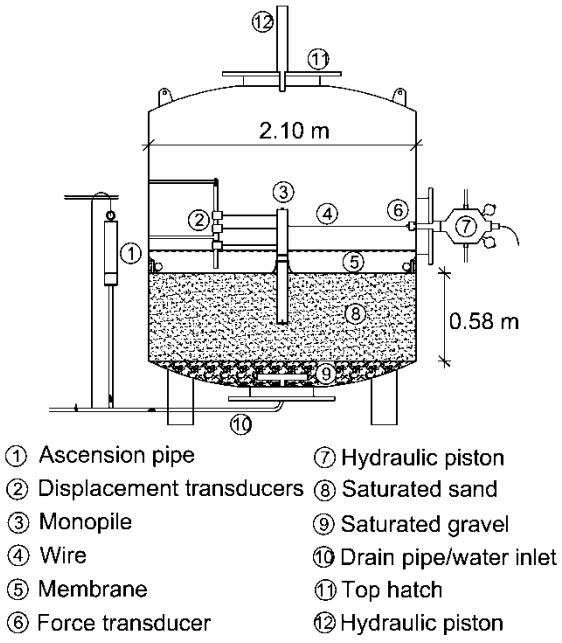

Figure 1. Cross sectional view of the pressure tank and the test setup.

3 TEST IN PRESSURE TANK

The tests are carried out in a pressure tank installed in the Geotechnical Engineering Laboratory at Aalborg University, Denmark. The tank has a height of 2.5 m and a diameter of 2.1 m. The tank is placed in a load-frame on a reinforced foundation separated from the rest of the floor in the laboratory.

3.1 Test Setup

Inside the tank, a 0.58 m thick layer of fully saturated sand with a layer of highly permeable gravel underneath is located. A cross sectional view of the pressure tank and test setup can be seen in Figure 1.

The test piles were installed in the sand layer and a lateral load was applied by means of a wire connected in series to a hydraulic piston through a force transducer.

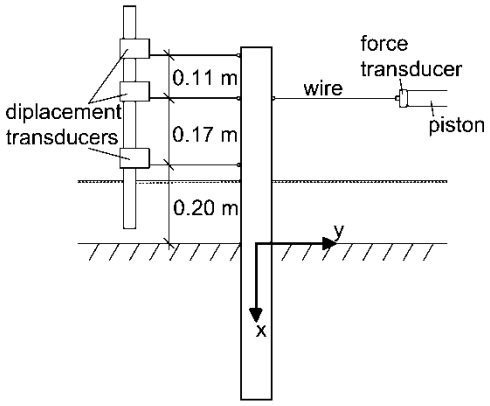

Figure 2. Setup for measuring the lateral deflection of the pile at three levels. The measurements are given in mm.

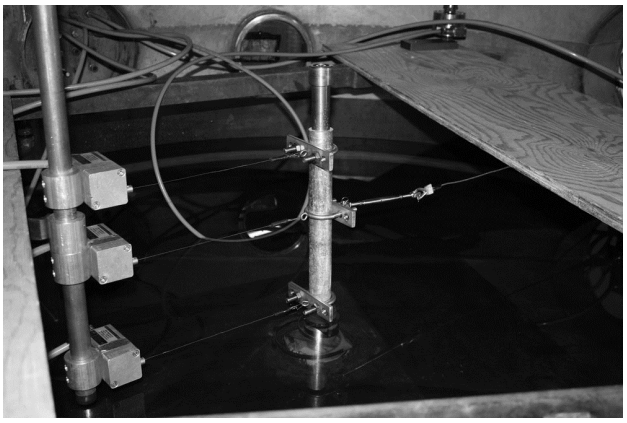

Figure 3. The 40 mm pile instrumented with three displacement transducers.

The deflection of the piles was measured by displacement transducers attached in three different levels above soil surface, cf. Figures 2 and 3. Thereby, three load-deflection relationships were obtained.

3.2 Increase of the Effective Stresses

The increase of the effective stresses in the soil was obtained by placing an elastic, rubber membrane on the soil surface. The membrane was placed around the pile and against the side of the tank causing the fully saturated soil to be sealed from the air in the upper part of the tank, cf. Figure 4. Water was poured in on top of the membrane to ensure fully saturated sand even if there were small gaps in the membrane or in the sealing between membrane and tank. Moreover, the dynamic viscosity of water is approximately 55 times greater than of air, and thereby the water minimized the flow through gaps.

Figure 4. The membrane placed on the soil surface and secured around the pile by hose clips and against the side of the tank by a fire hose.

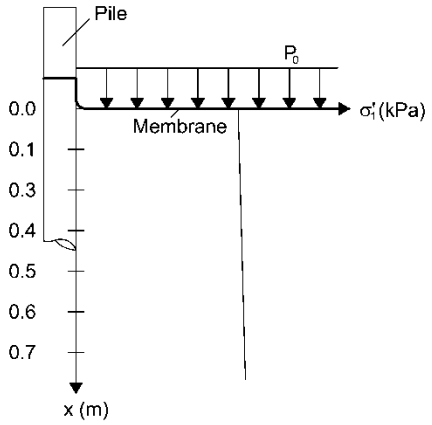

Figure 5. Effective vertical stresses in the soil when applying overburden pressure.

The effective stresses were then increased by closing the openings in the tank and applying an air pressure of 50 kPa and 100 kPa, respectively. Because the pressure in the upper part of the tank made the membrane resemble an applied surface load, a homogeneous increase of the effective stresses was obtained.

3.3 Hydrostatic Pore Pressure

To maintain a hydrostatic pore pressure in the soil, an ascension pipe was connected to the tank and, thereby, the water flowing through the gaps was led out of the tank. This way, the soil remained fully saturated and the stresses were applied as effective stresses only. The variation of the effective vertical stresses in the soil layer is shown in Figure 5, where P_0 denotes the applied overburden pressure.

4 MEASURING SYSTEM

The hydraulic piston used to actuate the pile was controlled by a predefined displacement ,and it acted at a vertical eccentricity of 370 mm above the soil surface, cf. Figure 2. The force transducer connecting the wire and the hydraulic system in series was a HBM U2B 10 kN for tests on the 40 mm pile and a HBM U2B 20 kN for the 100 mm pile.

The displacement transducers were of the type WS10-1000-R1K-L10 from ASM GmbH. For measuring the pressure in the tank, a HBM P6A 10 bar absolute pressure transducer was employed in the first test and a HBM P3MBA 5 bar absolute pressure transducer was employed in the remaining tests reducing the fluctuations of the measurements. The sampling frequency was 10 Hz.

5 SOIL CONDITIONS

The sand used in the tank was Baskarp Sand No. 15. The material properties for Baskarp Sand No. 15 are well-defined from previous tests in the laboratory at Aalborg University. A representative distribution of the grains found by sieve analysis is shown in Figure 6. The uniform grading of the grains makes it possible to obtain a homogeneous compaction of the soil. The hydraulic conductivity is $k = 6 \cdot 10^{-5}$ m/s. The loading velocity was $1 \cdot 10^{-5}$ m/s, thus, the soil was considered drained during the tests. The material properties for the sand are given in Table 2.

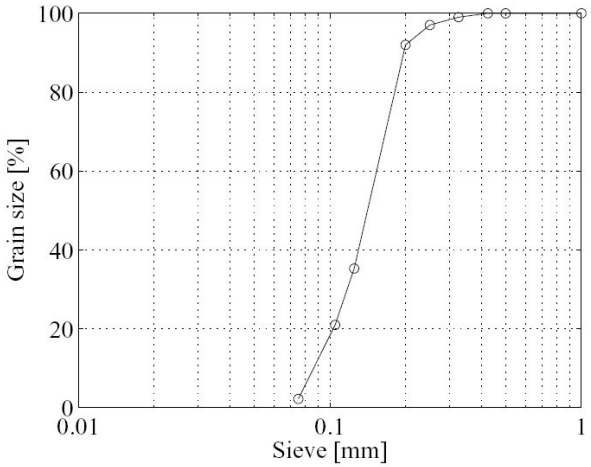

Figure 6. Distribution of Baskarp Sand No. 15 found by sieve analysis. (Ibsen and Bødker, 1994)

Table 2. Material properties for Baskarp Sand No. 15. (Andersen et al., 1998)

Specific grain density d_s [-]	Maximum void ratio e_{max} [-]	Minimum void ratio e_{min} [-]	50%-quantile d_{50} [mm]	Uniformity coefficient $U=d_{60}/d_{10}$ [-]
2.64	0.858	0.549	0.14	1.78

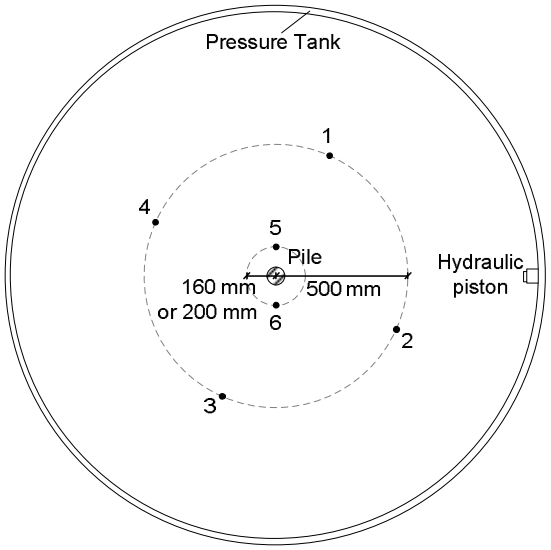

Figure 7. The positions of the six CPT's conducted prior to each test.

5.1 Soil Preparation

Prior to each test, the soil was loosened by an upward gradient of 0.9. Hereafter, it was vibrated mechanically to ensure fully saturated soil and a homogeneous compaction.

The pile was installed in the centre of the tank. During installation, a gradient of 0.9 was applied to minimise the pressure on the closed end of the pile. Hereby, the toe resistance and the skin friction along the pile were minimised. After the installation, the soil was vibrated mechanically to minimise disturbances in the soil emerged from the pile installation. While vibrating the soil, the pile was secured in its upright position by means of the hydraulic piston mounted through the top hatch of the tank, cf. Figure 1.

To control the homogeneity and the compaction of the soil, cone penetration tests (CPT) were conducted. A total of six CPTs were conducted prior to each test. Four were conducted at a distance of 500 mm from the centre of the pile, cf. Figure 7. The remaining two CPTs were conducted 160 mm and 200 mm from the pile centre for the 40 mm and the 100 mm pile, respectively. Both were conducted on the neutral side of the pile. The probe diameter of the CPT-devise was 15 mm.

In Figure 8 the cone resistance of the CPT's conducted prior to test 5 shows a homogeneous compaction of the soil. Figure 9 shows the mean value of the cone resistance, q_c, prior to each of the six tests described in this paper and those obtained prior to the tests described in Sørensen et al. (2009). The figure shows that q_c of the soil was approximately the same for the six tests conducted on the 40 mm pile and the 100 mm pile. Though, compared to the CPT's conducted in Sørensen et al. (2009) they were higher.

In Table 3 the soil parameters derived on basis of the CPT's are presented. The parameters are derived in accordance to Ibsen et al. (2009), cf. Equations 1 to 5, which are derived empirically for Baskarp Sand No. 15. The formulation for the tangential modulus of elasticity, E_0 cf. Equation 6, is given by Brinkgreve and Swolfs (2007).

$$\varphi_{tr}=0.152I_D+27.39\sigma_3^{'\,-0.2807}+23.21 \quad [1]$$

$$\psi_{tr}=0.195I_D+14.86\sigma_3^{'\,-0.09764}-9.946 \quad [2]$$

$$I_D=c_2\left(\frac{\sigma_1^{'}}{(q_c)^{c_1}}\right)^{c_3} \quad [3]$$

$$\gamma^{'}=\frac{d_s-1}{1+e_{in\text{-}situ}}\gamma_w \quad [4]$$

$$E_{50}=\left(0.6322I_D^{2.507}+10920\right)\left(\frac{c\cos\varphi_{tr}+\sigma_3^{'}\sin\varphi_{tr}}{c\cos\varphi_{tr}+\sigma_3^{'\,ref}\sin\varphi_{tr}}\right)^{0.58} \quad [5]$$

$$E_0=\frac{2E_{50}}{2-R_f} \quad [6]$$

φ_{tr} is the internal angle of friction, I_D is the identity index, σ_3' and σ_1' are the effective horizontal and vertical stresses, respectively, and φ_{tr} is the dilation angle. (c_1, c_2, c_3) = (0.75, 5.14, -0.42), γ' is the effective unit weight of the soil, d_s is the relative density of the soil, $e_{in\text{-}situ}$ is the in-situ void ratio, and w is the unit weight of water. E_{50} is the secant modulus of elasticity, c is the cohesion, and R_f is the failure ratio, which is normally set to 0.9.

By comparing the obtained parameters to the ones derived in Sørensen et al. (2009), given in Table 4, the identity indices, I_D, derived for the present tests are noted as approximately 10 % higher. Because the internal angle of friction, φ_{tr}, and the effective unit weight of the soil, γ', are dependent on I_D these parameters are slightly higher as well. The tangential modulus of elasticity, E_0, is not calculated for the tests without overburden pressure because the low stress level leads to large uncertainties in the determination.

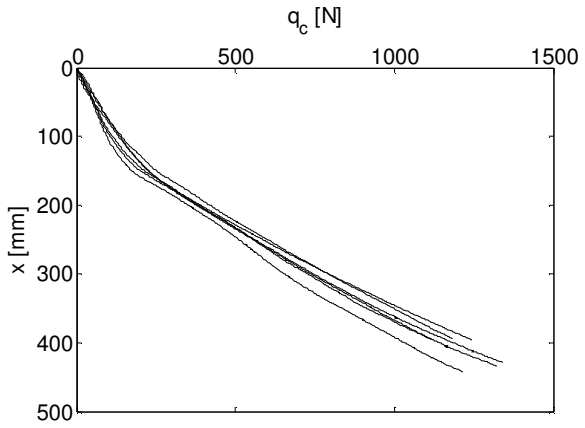

Figure 8. The cone resistance, q_c, from the CPT's conducted prior to test 5.

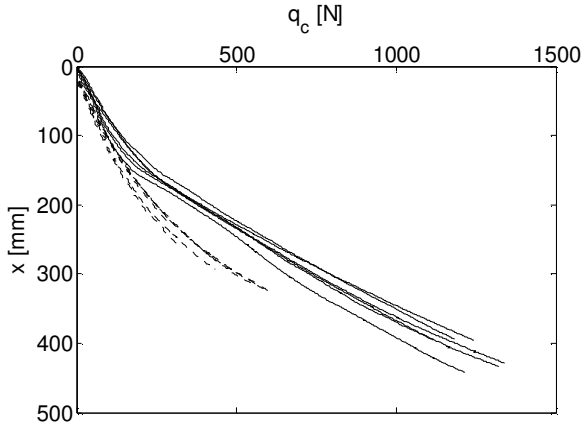

Figure 9. Mean values of the cone resistance, q_c, prior to each test. The solid curves are q_c obtained prior to the tests described in this paper. The dashed curves are q_c obtained prior to the tests described in Sørensen et al. (2009).

6 RESULTS

During the tests, prescribed displacements were applied to the pile and, thereby, the soil was brought to failure, then unloaded and reloaded. Hereby, an estimation of the ultimate soil resistance and the elastic behaviour of the soil can be obtained.

In Figure 10, the load-deflection relationships for test 4 are shown. Firstly, it can be seen that, when unloading and reloading, the load-deflection curves reach the original curves. Secondly, the upper displacement transducer recorded the largest deflection, while the lower transducer recorded the smallest. This is in agreement with the expected results.

Table 3. Material properties determined from the CPTs conducted prior to the six tests.

D [mm]	P_0 [kPa]	φ_{tr} [°]	ψ_{tr} [°]	I_D [-]	γ' [kN/m^3]	E_0 [MPa]
100	0	53.8	19.6	0.86	10.3	-
100	50	50.3	19.0	0.89	10.4	38.2
100	100	47.7	18.3	0.90	10.4	55.6
40	0	54.4	20.4	0.91	10.4	-
40	50	50.4	19.1	0.89	10.4	38.6
40	100	48.0	18.6	0.91	10.4	57.2

Table 4. Material properties determined from the CPTs conducted prior to the six tests conducted in Sørensen et al. (2009).

D [mm]	P_0 [kPa]	φ_{tr} [°]	ψ_{tr} [°]	I_D [-]	γ' [kN/m^3]	E_0 [MPa]
60	0	52.6	18.1	0.79	10.2	-
60	50	48.5	16.9	0.79	10.2	25.4
60	100	45.9	16.2	0.79	10.2	41.1
80	0	52.2	17.5	0.76	10.1	-
80	50	48.3	16.7	0.78	10.1	24.9
80	100	45.1	15.3	0.75	10.1	37.4

11. The test without overburden pressure gives a more curved graph than the tests with overburden pressures. This is caused by the low stress level, at which the dilation of the soil is larger.

6.1 Plastic Response and Pile Capacity

The plastic behaviour of the soil depends on the applied overburden pressure. For the case without overburden pressure the plastic deformation after the first unloading is approximately 85 % of the total deformation after the first loading. For the cases where overburden pressures of 50 kPa and 100 kPa are applied, the plastic deformation is 50 % and 60 %, respectively, of the total deformation after the first loading, cf. Figure 11.

In Figure 11, several loading-reloading curves are observed as present for the test at 50 kPa. The reason for this deviation compared to the remaining tests is that the test was run in three stages because of problems with the wire transferring the load to the pile.

Figures 12 and 13 present the dependency of the overburden pressure on the lateral load. As expected, the capacity of the soil increases with increasing overburden pressure. The difference between the lateral loads for the tests without overburden pressure compared to the ones with overburden pressures is determined for a deflection of 10 mm at the level of the hydraulic piston. For an overburden pressure of 50 kPa, the lateral load increases with a factor of 17 for the 40 mm pile and with a factor of 14 for the 100 mm pile. For an overburden pressure of 100 kPa, the lateral load increases with a factor of 18 for the 40 mm pile and with a factor of 20 for the 100 mm pile.

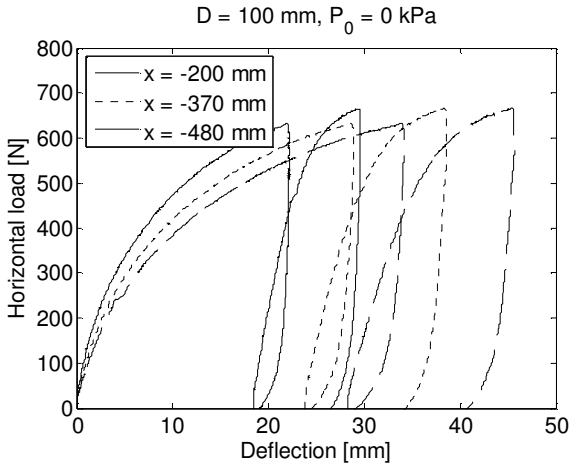

Figure 10. Load-deflection relationships for the 100 mm pile at P_0 = 0 kPa.

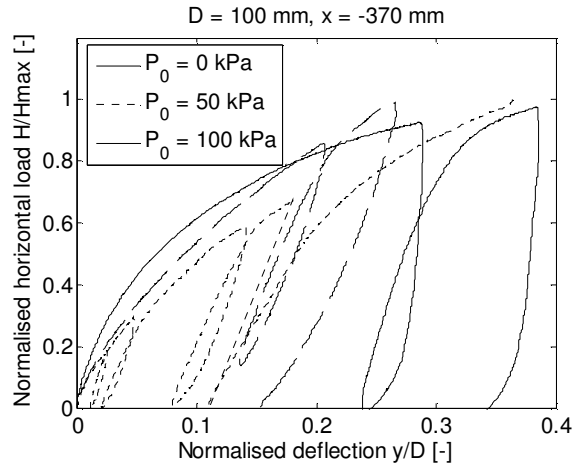

Figure 11. Normalised load-deflection relationships measured at the height of the hydraulic piston (x = –370 mm) for the 100 mm pile.

6.2 Uncertainties for the 40 mm Pile

Conducting tests on the 40 mm pile was difficult because small disturbance of the soil would cause large uncertainties for the obtained results due to the small soil volume activated during failure. Figure 12 shows the load-deflections relationship for the 40 mm pile. The figure shows an unexpected appearance on the graph for the test at 100 kPa as the graph for the first loading has a nearly straight line. Before this test, the pile got stuck in the hydraulic piston. When it was released it the surrounding soil was disturbed, this might have caused a decrease of the soil strength. So, the graph is straight till the point where the pile obtained a deflection large enough to activate the undisturbed soil. Therefore, the results from test 6 are considered to be representative of the behaviour of undisturbed soil.

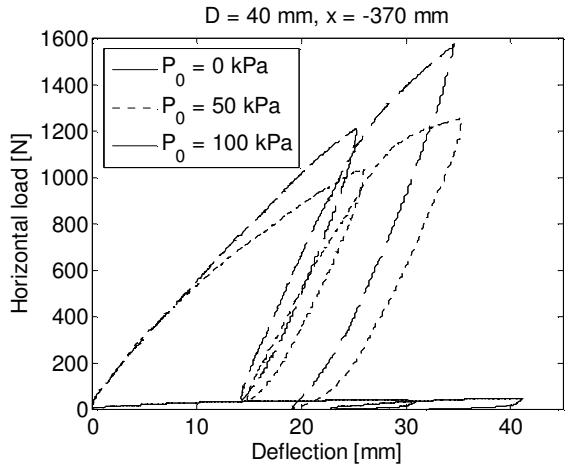

Figure 12. Load-displacement relationships at different overburden pressures measured at the level of the hydraulic piston (x = –370 mm) for the 40 mm pile.

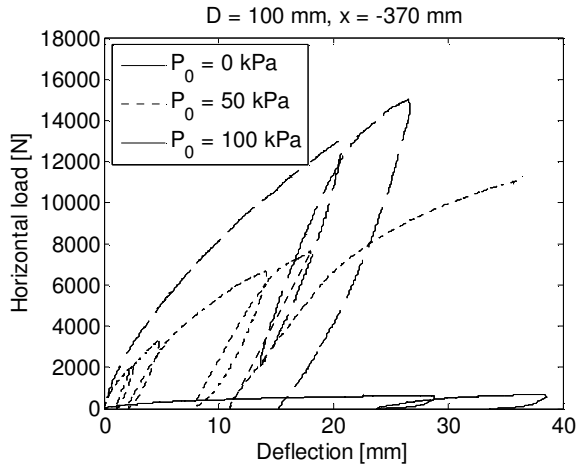

Figure 13. Normalised load-deflection relationships measured at the level of the hydraulic piston (x = –370 mm) for the 100 mm pile.

6.3 Comparison of Test Results

In Figure 14, the results of the tests without overburden pressure are compared to the results obtained by Sørensen et al. (2009) for 60 mm and 80 mm piles. As expected, the lateral load necessary to obtain a deflection of the pile increases with increasing pile diameter. Figures 15 to 17 shows the normalized relationships between the lateral load, H, and the deflection, y, determined at the level of the hydraulic piston for the three stress levels. The normalised formulation of the load, Equation 7, is chosen because the load is assumed to be dependent on the soil volume activated during failure and the stresses in the soil. This assumption provides the expression $LD\sigma'$ that can be rewritten to $LD\gamma'L = L^2D\,\gamma'$.

$$\text{Normalised load} = \frac{H}{L^2 D \gamma'} \quad [7]$$

$$\text{Normalised deflection} = \frac{y}{D} \quad [8]$$

Figure 15 shows deviations between the normalized curves for the four piles without overburden pressure. The curves seem to be grouped in pairs. The 80 mm pile and the 100 mm pile are similar at the initial part of the curves, but deviate at larger deflections. The curves for the 40 mm and the 60 mm pile are similar, but this might be caused by the fact that the identity index for the soil was approximately 10 % larger in the test on the 40 mm pile than in the test on the 60 mm pile, cf. Tables 3 and 4.

The reason for the deviations could be the difference in the soil volume activated during failure and the different embedded lengths for the four piles, which causes deviations in the reached stress levels.

In Figure 16, the initial parts of the graphs are noted as almost similar when applying an overburden pressure of 50 kPa. The smaller deviations indicate that the accuracy of the results increases when overburden pressure is applied. For the tests with overburden pressure of 100 kPa, the curves are coinciding for the tests on the 60 mm, 80 mm, and 100 mm piles. This implies that the accuracy of the test results increases with increasing overburden pressure. The deviation of the curve for the 40 mm pile is caused by the disturbance of the soil before the test.

In spite of the inaccurate results for the tests without overburden pressure and for the tests of the 40 mm pile, the normalized relationships indicate that the lateral load is proportional to the embedded length squared and the pile diameter, cf. Equation 7. Furthermore, they indicate that the accuracy of small-scale testing increases with increasing overburden pressure.

7 CONCLUSION

The paper presents results from six small-scale quasi-static tests on laterally loaded piles in sand. The piles had outer diameters of 40 mm and 100 mm, respectively, and a slenderness ratio, L/D, of 5. The tests were conducted in a pressure tank with various overburden pressures.

By increasing the effective stresses in the soil the problems with the non-linear yield surface for small stress levels were avoided. The increase of the effective stress levels were successfully obtained by separating the sand from the upper part of the tank by an elastic membrane.

The problems with the non-linear yield surface were seen in the results for the tests without overburden pressure, as the curves for the normalised relationships were not similar. The similarity for the normalized results were obtained for the tests with overburden pressure of 100 kPa, and it can be concluded that accuracy in small-scale testing increases with increasing overburden pressure. Therefore, it is recommended to conduct small-scale tests with higher overburden pressure applied in future research.

The uncertainties when conducting tests on the 40 mm pile were high, because small disturbances of the soil led to results in disagreement to the other test results. Consequently, it is difficult to draw reasonable conclusions from these tests. In further research small-scale tests should be conducted on piles with larger diameters.

The test results obtained for the 100 mm pile and the test results obtained by Sørensen et al. (2009) both indicate that the lateral load acting on the pile is proportional to the embedded length squared times the pile diameter.

ACKNOWLEGDEMENTS

The project is associated with the EFP programme “Physical and numerical modelling of monopile for offshore wind turbines”, journal no. 033001/33033-0039 and the EUDP programme “Monopile cost reduction and demonstration by joint applied research”. The funding is sincerely acknowledged.

REFERENCES

Andersen, A., Madsen, E. and Schaarup-Jensen 1998. Eastern Scheldt Sand, Baskarp Sand No. 15, *Data Report 9701 Part 1*, Aalborg University, Denmark.

API 1993. *Recommended Practice for Planning, Designing and Constructing Fixed Offshore Platforms - Working Stress Design*, American Petroleum Institute.

Brødbæk, K., Møller, M., Sørensen, S. and Augustesen, A. 2009. Evaluation of p-y relationship in cohesionless soil, *DCE Technical Report No. 57,* Aalborg University, Denmark.

Brinkgreve, R. B. J. and Swolfs, W. 2007. *PLAXIS 3D FOUNDATION Material Models manual Version 2*, Plaxis bv, Delft, Netherlands

DNV 1992. *Det Norske Veritas -Foundations*, Det norske veritas Classification A/S, Høvik, Norway.

Ibsen, L. B., Hanson, M., Hjort, T. And Thaarup, M. 2009. MC-Parameter Calibration for Baskarp Sand No. 15, *DCE Technical Report No. 62*, Aalborg University, Denmark.

Ibsen, L. and Bødker, L. 1994. Baskarp Sand No. 15, *Data Report 9301,* Geotechnical Engineering Group, Aalborg University, Denmark

Sørensen, S., Brødbæk, K., Møller, M., Augustesen, A. and Ibsen, L. 2009. Evaluation of the Load-Displacement Relationships for Large-Diameter Piles in Sand, *Civil-Comp Press*, Paper 244.

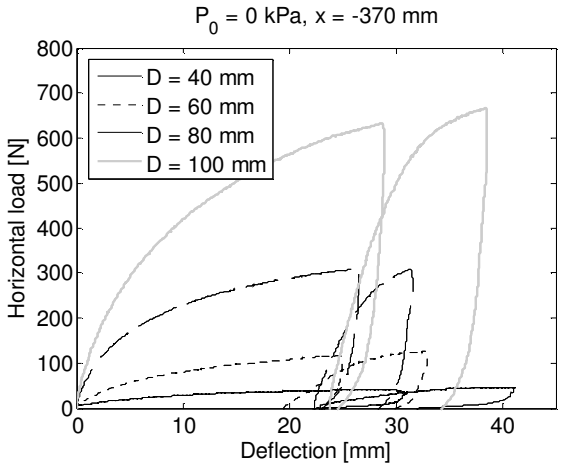

Figure 14. Load-deflection relationships for the four piles at P_0 = 0 kPa.

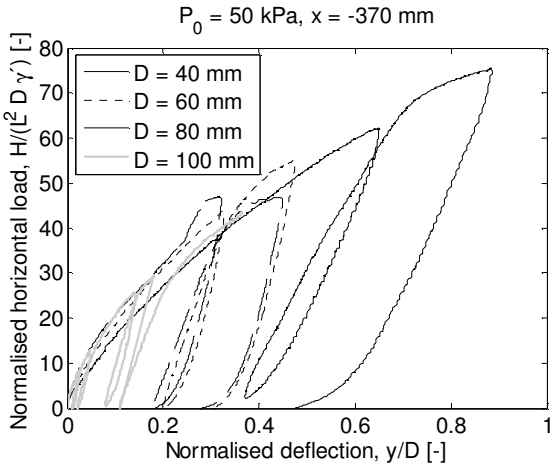

Figure 16. Normalised relationships between load (H/H_{max}) and deflection (y/D) measured at the level of the hydraulic piston for the tests at P_0 = 50 kPa.

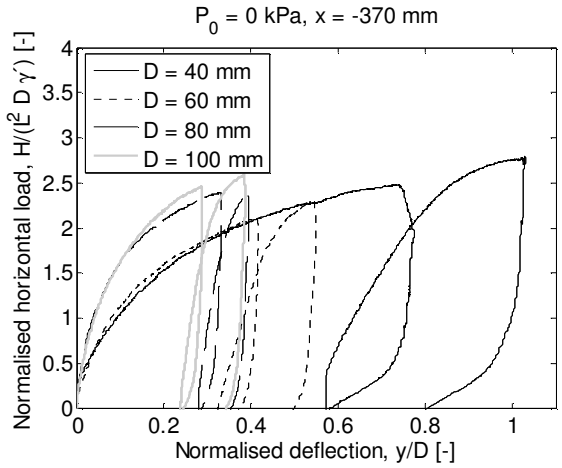

Figure 15. Normalised relationships between load (H/H_{max}) and defection (y/D) measured at the level of the hydraulic piston for the tests at P_0 = 0 kPa.

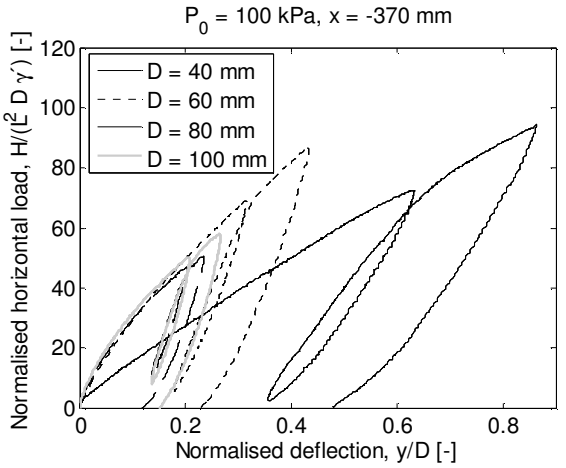

Figure 17. Normalised relationships between load (H/H_{max}) and deflection (y/D) measured at the level of the hydraulic piston for the tests at P_0 = 100 kPa.